Available online at www.sciencedirect.com

ScienceDirect

Energy Procedia 45 (2014) 938 – 948

Energy Procedia

68th Conference of the Italian Thermal Machines Engineering Association, ATI2013

A Tridimensional CFD Analysis of the Oil Pump of an High Performance Motorbike Engine

Emma Frosina[a,]*, Adolfo Senatore[a,], Dario Buono[a,]

[a]*Department of Industrial Engineering, University of Naples Federico II, Via Claudio 21, Naples 80125, Italy*

Mario Unicini Manganelli[b,]

[b]*Aprilia Racing- Gruppo Piaggio & C. S.p.A., Aprilia, Italy*

Micaela Olivetti[c,]

[c]*OMIQ s.r.l., Via Lattuada, 31, Milan 20135, Italy*

Abstract

The main target of nowadays engine designers is to focus on exhaust emissions, fuel consumption and engine performance, so during the design phase of a new internal combustion engine, all the aspects related to friction and mechanical power loss must be deeply considered. And then, also the friction related to engine lubrication system must be analyzed and studied.

In this paper a tridimensional CFD analysis of the lubrication circuit oil pump of a modern high-performance engine manufactured by Aprilia will be shown. The model was build up with PumpLinx®, a commercial CFD 3D code by Simerics Inc.®, taking into account all the phenomena associated to the fluid cavitation. The model was validated by data of an experimental campaign performed on a hydraulic test bench, at the Industrial Engineering Department of the University of Naples, Federico II.

Keywords: 3D CFD, oil pump modeling of lubrication circuit

* Corresponding author.
E-mail address: emma.frosina@unina.it

doi:10.1016/j.egypro.2014.01.099

1. Introduction

Internal combustion engines have now achieved the objective of high specific power output with low fuel consumption and low exhaust gas emissions [1]. Consequently, engine running conditions have become very onerous and engines have to ensure good performance on a wide range of operating points. Hence all engine components have to be carefully studied and designed from the early stages of their development.

The oil delivery pump is, by all means, one of the components that can be analyzed to reduce mechanical power losses. In effect, the main drawback of fixed displacement pumps is power losses due to the flow-rate recirculation within the pressure relief valve, especially at high shaft rotational speed. Such an excess flow-rate is due to the pumps size selection process, which focuses on providing the necessary flow-rate at low regimes.

In recent years, during the design phase, one - dimensional and three - dimensional codes have been used to simulate the behavior of the oil circuit components. Using these codes, information may be obtained on points that are not always experimentally measurable. 1D codes are simpler to use for modeling complex systems and require less computational power. On the other hand, they can hardly be predictive as 3D codes.

This paper focuses on the modeling of an oil delivery pump with a CFD three - dimensional code. A model validation exercise has been performed comparing CFD results with experimental data obtained at the Department of Industrial Engineering of University of Naples “Federico II”.

2. Engine and pump description

In this paper it we present the oil pump of a high performance motorbike engine manufactured by Aprilia (see figure 1), four cylinders with a displacement of 999,6 cm^3, and a maximum rotation speed of 14000 rpm. The lubrication circuit is a wet sump type and is fed by a gerotor volumetric pump, with a displacement of 8 cm^3/rev.

Fig 1. Motorbike engine

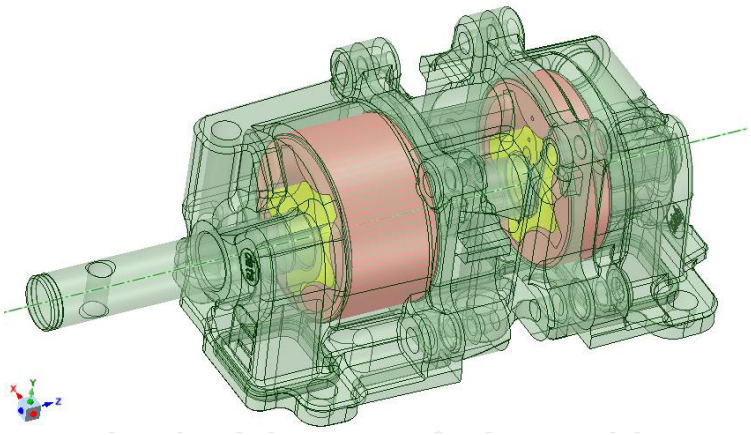

Fig 2. Pump rotors

The lubrication pump consists of two gears (figure 2), with the inner rotor rotating off - center, creating 5 vanes with volumes evolving in one revolution from a minimum to a maximum value during the suction phase and vice versa during the discharge phase.

The rotors have 4 and 5 teethes respectively, the outer rotor rotates with an angular velocity that is equal to 4/5 of the inner rotor velocity (the transmission ratio between the rotors is 4/5).

The whole pump consists in fact of two (twin) pumping units as it is used also for the oil cooling circuit (as showed in figure 2).

In this paper, we present the whole pump model (for the lubrication and oil cooling circuit) and the validation of the lubrication pump model.

3. Pump model

The pump has been simulated with a commercial CFD 3D code PumpLinx® by Simerics Inc.®, that solves numerically the fundamental conservation equations of mass, momentum and energy and includes accurate physical models for turbulence and cavitation.

From the pump 3D CAD geometry, the fluid volume has been extracted, starting from the surfaces wet by the lubricant itself. The obtained geometry has then been meshed with the program grid generator [4].

Figure 3 shows the pump mesh in a section plane of the considered pump. In the boundary layer we have increased the grid density on the surface without excessively increasing the total cell count. In the regions of high curvature and small details, the grid has been subdivided and cut to conform to the surface.

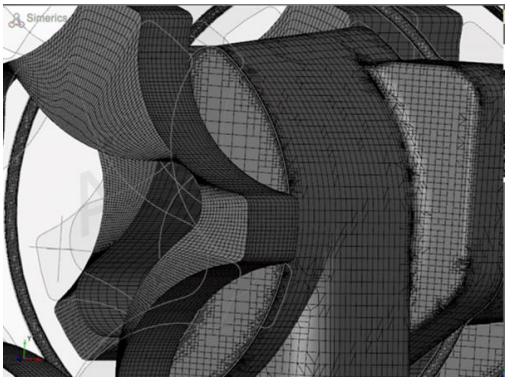

Fig. 3. Binary Tree Mesh – pump cross section

As already mentioned, the code solves, during the simulations, the conservation equations of mass, momentum and energy:

Mass Conservation

$$\frac{\vartheta}{\vartheta t}\int_{\Omega(t)}\rho d\Omega + \int_{\sigma}\rho(v - v_{\sigma})\,n d\sigma = 0 \tag{1}$$

Momentum Conservation

$$\frac{\vartheta}{\vartheta t}\int_{\Omega(t)}\rho v d\Omega + \int_{\sigma}\rho\big((v - v_{\sigma})n\big)\,v d\sigma = \int_{\sigma}\tilde{\tau} n d\sigma - \int_{\sigma} p n d\sigma + \int_{\Omega} f d\Omega \tag{2}$$

Energy Conservation

$$\frac{\vartheta}{\vartheta t}\left[\rho\left(u + \frac{v^2}{2} + gz\right)\right] + \nabla\left[\rho v\left(h + \frac{v^2}{2} + gz\right)\right] + \nabla Q - \nabla(T_d v) = 0 \tag{3}$$

in which $\Omega(t)$ is the control volume, σ is the control volume surface, n is the surface normal pointed outwards, ρ is the fluid density, p is the pressure, f is the body force, v is the fluid velocity, v_{σ} is the surface motion velocity. The shear stress tensor $\tilde{\tau}$ is a function of the fluid viscosity μ and of the velocity gradient; for a Newtonian fluid, this is given by the following equation:

$$\tau_{ij} = \mu\left(\frac{\vartheta u_i}{\vartheta x_j} + \frac{\vartheta u_j}{\vartheta x_i}\right) - \frac{2}{3}\mu\frac{\vartheta u_k}{\vartheta x_k}\delta_{ij} \tag{4}$$

Where u_i (i = 1,2,3) is the velocity component e δ_{ij} is the Kronecker delta function.

The code allows for the simultaneous treatment of moving (rotors) and stationary (intake and delivery ports) fluid volumes. Each volume connects to the others via an implicit interface.

Different techniques are available for the treatment of a moving mesh. For positive displacement pumps, it is necessary to use a moving/sliding methodology whereby the stationary and moving volumes are meshed separately. Each moving volume connects to the others via a common interface, which, due to deformations and motion, is updated at each time-step.

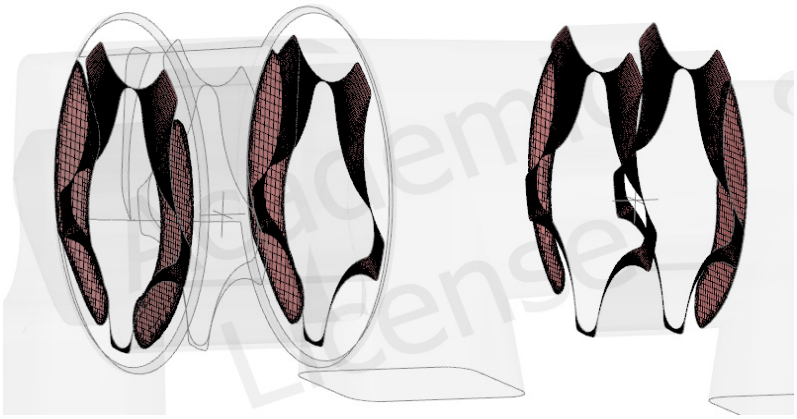

Fig. 4. Mismatched Grid Interface between the end of two offset cylinders

The model of the considered pump consists of a 400.000 cells mesh. The following figures show section cuts that illustrate the grid differences between stationary and moving parts.

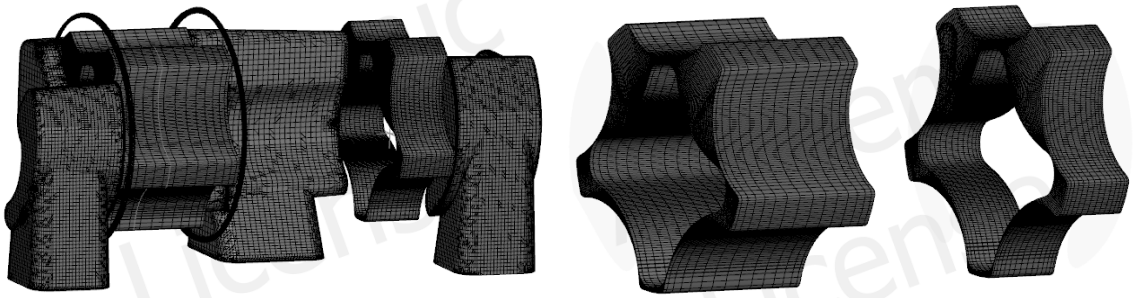

Fig 5. Pump and Rotors mesh

This CFD 3D code can also implement a real fluid model based on the work of Singhal [5] [10] [12], and therefore allows for the calculation of cavitation effects, when pressure in a specified zone of the fluid domain falls below the saturation pressure. Vapour bubbles form and then collapse as the pressure rise again [4] [7] [8].

Many physical models for the formation and transport of vapour bubbles in the liquid are available in literature, but only few computational codes offer robust cavitation models. This is due to the difficulty to handle gas/liquid mixtures with very different densities. Even small pressure variations may cause numerical instability if they are not optimally treated [7].

The cavitation model implemented in the code uses the following equations:

$$\frac{\vartheta}{\vartheta t}\int_{\Omega(t)}\rho f d\Omega + \int_{\sigma}\rho\big((v-v_{\sigma})n\big)f d\sigma = \int_{\sigma}\left(D_f + \frac{\mu_t}{\sigma_f}\right)(\nabla f n)\,d\sigma + \int_{\Omega}(R_e - R_c)d\Omega \qquad (5)$$

where D_f is the diffusivity of the vapour mass fraction and σ_f is the turbulent Schmidt number. In the present study, these two numbers are set equal to the mixture viscosity and unity, respectively [4].

The code fluid model accounts for liquid compressibility. This is critical to accurately model pressure wave propagation in liquid. The liquid compressibility is found very important for a high pressure system and the systems in which water hammer effects are relevant.

The software implements mature turbulence models, such as the standard $k-\varepsilon$ model and RNG $k-\varepsilon$ model [11]. These models have been available for more than a decade and have been widely demonstrated to provide good engineering results. The standard $k-\varepsilon$ model, used for the simulations presented in this paper is based on the following two equations [11]:

$$\frac{\vartheta}{\vartheta t}\int_{\Omega(t)}\rho k d\Omega + \int_{\sigma}\rho\big((v-v_{\sigma})n\big)\,k d\sigma = \int_{\sigma}\left(\mu+\frac{\mu_t}{\sigma_k}\right)(\nabla k n)\,d\sigma + \int_{\Omega}(G_t-\rho\epsilon)d\Omega \quad (6)$$

$$\frac{\vartheta}{\vartheta t}\int_{\Omega(t)}\rho\epsilon d\Omega + \int_{\sigma}\rho\big((v-v_{\sigma})n\big)\,\varepsilon d\sigma = \int_{\sigma}\left(\mu+\frac{\mu_t}{\sigma_\varepsilon}\right)(\nabla\epsilon n)\,d\sigma + \int_{\Omega}\left(c_1 G_t\frac{\varepsilon}{k}-c_2\rho\frac{\varepsilon^2}{k}\right)d\Omega \quad (7)$$

With $c_1 = 1.44$, $c_2 = 1.92$, $\sigma_k = 1$, $\sigma_\varepsilon = 1.3$; where σ_k e σ_ε are the turbulent kinetic energy and the turbulent kinetic energy dissipation rate Prandtl numbers.

Boundary conditions were obtained from experimental data originated by a test bench campaign held at the Department of Industrial Engineering of University of Naples “Federico II”. In particular, suction port pressure and lubricant density as a function of rotational speed were provided as input for the numerical model, between 1000 rpm and 4000 rpm and with an oil temperature of 80°C and 110°C.

Once created the model, a large number of simulations has been run to obtain the pump characteristics map, which is delivery flow-rate as a function of pressure. Figure 6 show the pressure distribution in the pumping volume and the ports.

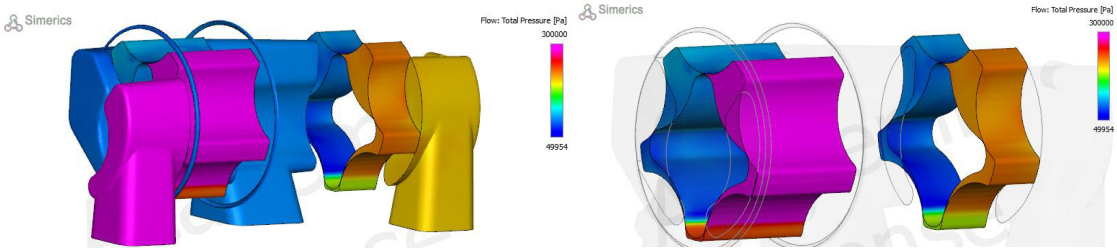

Fig 6. Pressure distribution in the fluid volume and in the the pumping volume (in between rotors)

4. Pump model validation

The pump model validation has been performed, as already mentioned, using data from an experimental campaign held at the Department of Industrial Engineering of University of Naples “Federico II”. The test bench hydraulics scheme is represented in figure 7, which will be used to describe the bench functionality.

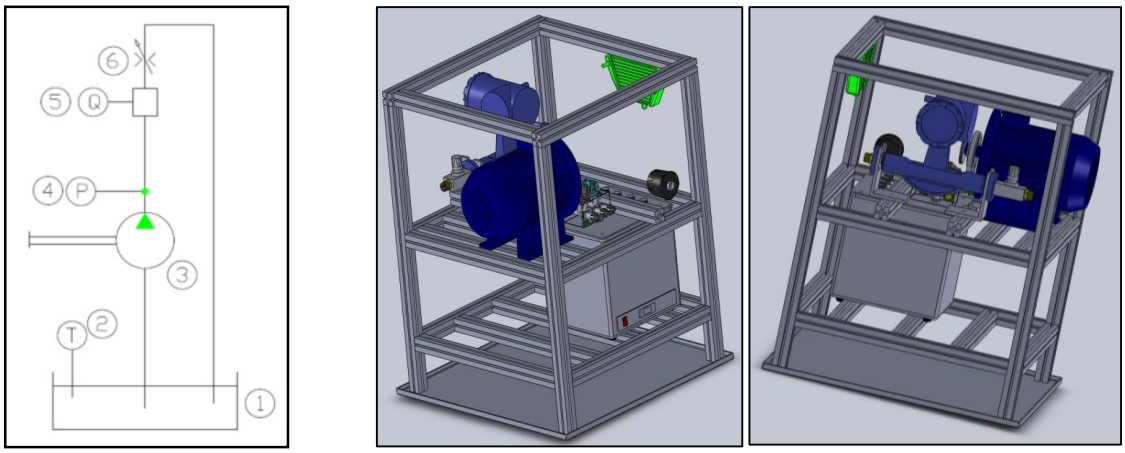

Fig 7. Pump test bench

The oil pump (3) draws oil from a thermostatic tank (1) and delivers it to a mass flow-rate transducer (5) and a lamination valve (6). In the test bench circuit, a thermocouple (2) and a pressure transducer (6) are also integrated in the bench. The pump is motored by an electric motor, which, through an inverter, can vary the pump shaft speed; acting on the lamination valve, the oil pressure in the delivery line can be changed. The pump speed is acquired thanks to a 360-teeth encoder.

The mass flow-rate transducer is a Proline Promass 83F, manufactured by Endress®, with the following characteristics:

- Measure principle: Coriolis effect;
- Max flow-rate: 6500 kg/h;
- Max error: 1% FS.

The pressure transducer (type LP11DA), manufactured by AVL®, has the following characteristics:

- Measure principle: Piezoresistive;
- Range: 0 – 10 bar;
- Sensitivity: 930 mV/bar.

The pressure transducer (type RS461-373 Gems®), has the following characteristics:

- Measure principle: strain gauge;
- Range: 0 – 10 bar;
- Precision: ±0.25%.

An acquisition system allows to control and manage the test bench output signals via a multi-function National Instruments® card (type NI PCI MIO 16 E 1) and a software tool for the management and acquisition of data based on LabView 2011 and developed at the Department of Industrial Engineering of University of Naples "Federico II".

The oil was a 5W40 that complies with API SL, JASO MA-2, and ACEA A3 specifications.

The tests allowed to determine the full pump characteristics map, in terms of pressure/flow-rate curves (figure 8) as a function of rotation speed and oil temperatures of 100°C.

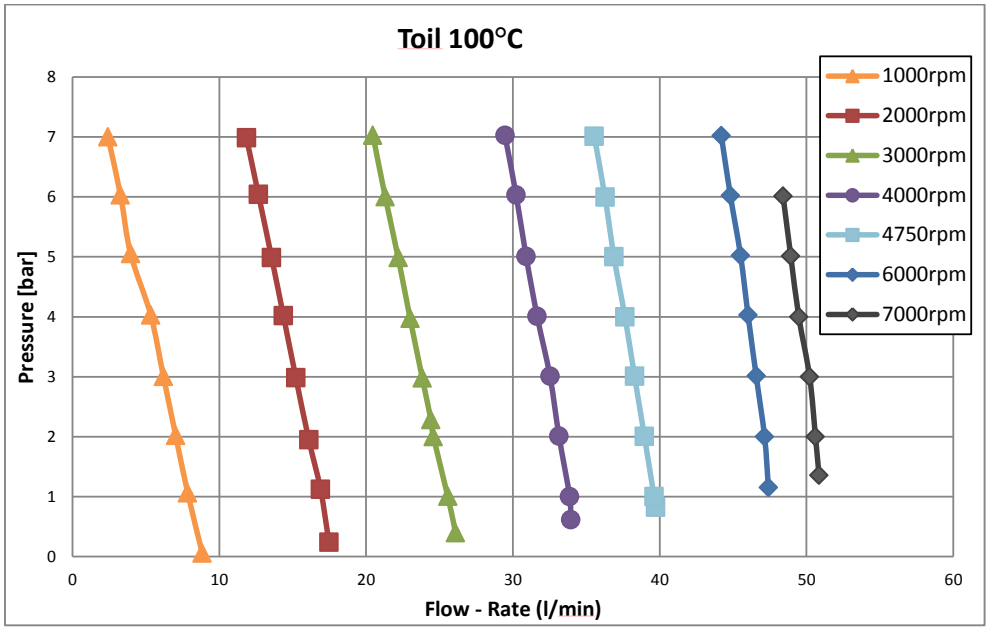

Fig 8. P-Q Curves at 100°C oil temperature

The following figure shows the flow-rate trend in function of engine speed between 1000 – 7000 rpm and oil pressure of 1bar, 3bar, 5bar and 7bar. The experimental curves here been compared with the theoretical curve.

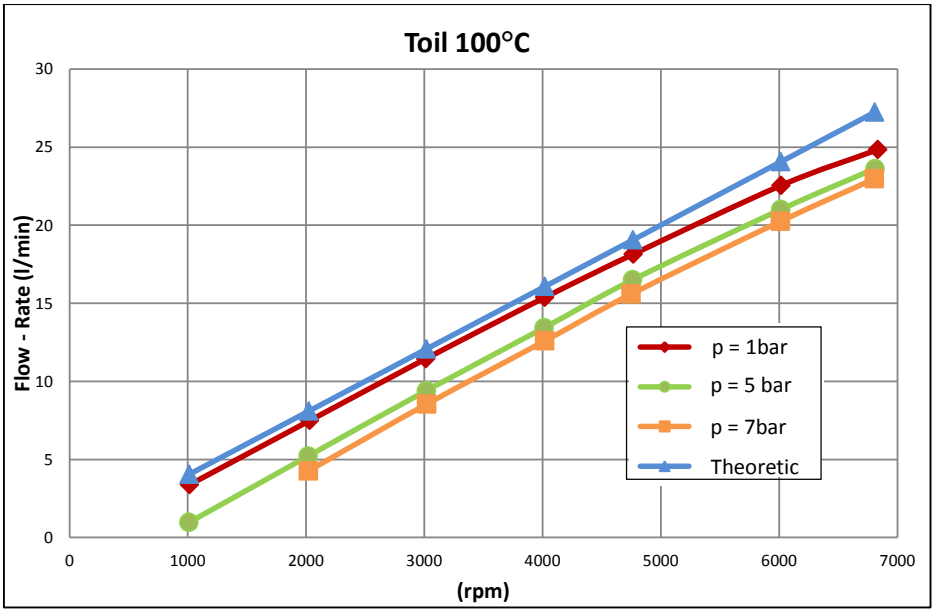

Fig 9. Q/rpm Curves

From the analysis of the above graph it can be noted that the slope of the experimental curves is very similar to the theoretical curve especially at low rotation speed.

The theoretical curve has been obtained from the following expression:

$$Q_{teo} = V_g \cdot \frac{n}{1000} \tag{8}$$

Where:

V_g is the displacement [cm^3];
n is the pump rotation speed [rpm];
Q is the pump flow-rate [l/min].

The pump efficiency has been calculated with the equation:

$$\eta = \frac{Q_{eff}}{Q_{teo}} \tag{9}$$

Where Q_{eff} is determined from experimental data.

The following graph shows the pump efficiency as function of rotation speed and oil pressure at the lubricant temperature of 100°C.

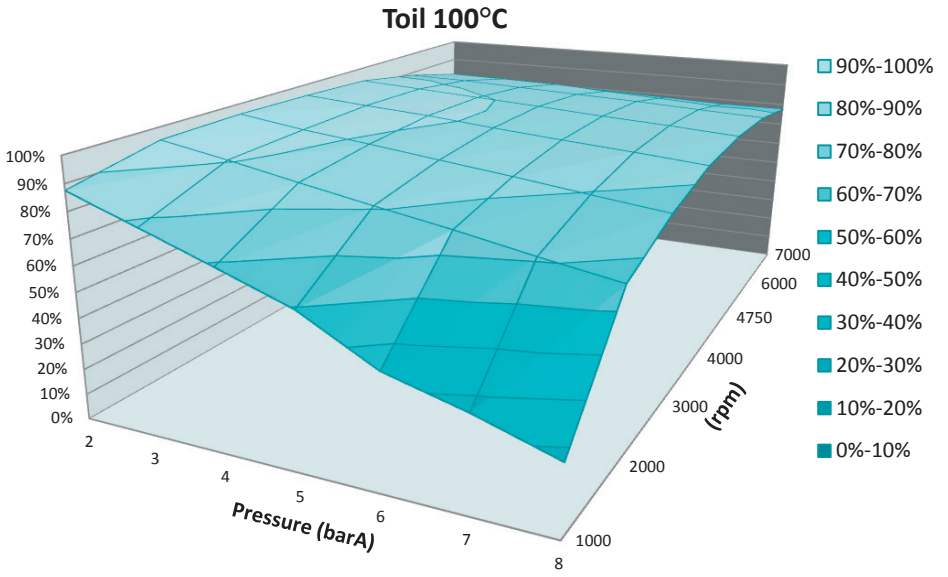

Fig 10. Oil pump efficency 100°C oil temperature

The full pump characteristics map has subsequently been calculated in terms of pressure/flow-rate curves (figure 11) as a function of rotation speed and oil temperatures of 80°C and 100°C.

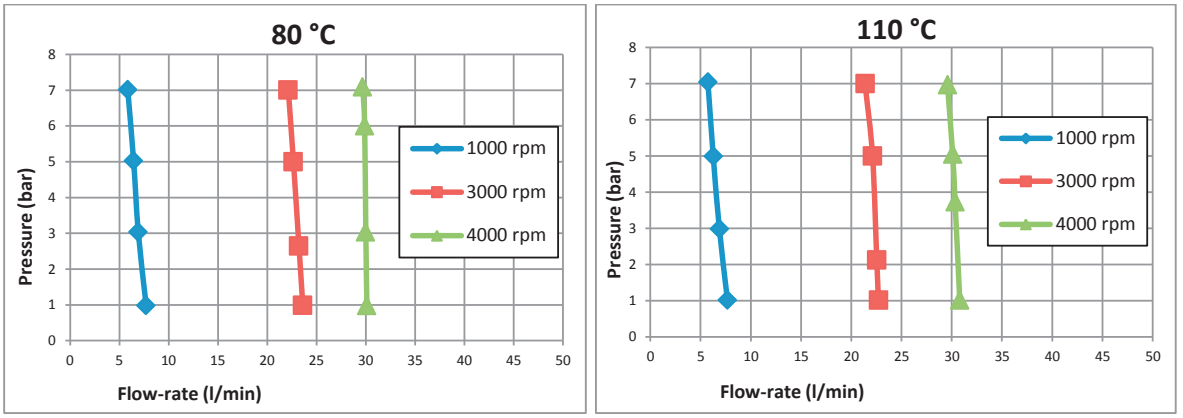

Fig 11: P-Q Curves at 80°C and 110°C oil temperature

The model validation has been carried out comparing results from the CFD 3D code simulations with experimental data at the different rotation speeds and oil temperatures (80°C and 110°C). Plots in figure 12 show the comparison between numerical model results (dashed lines) and experiments (continuous line).

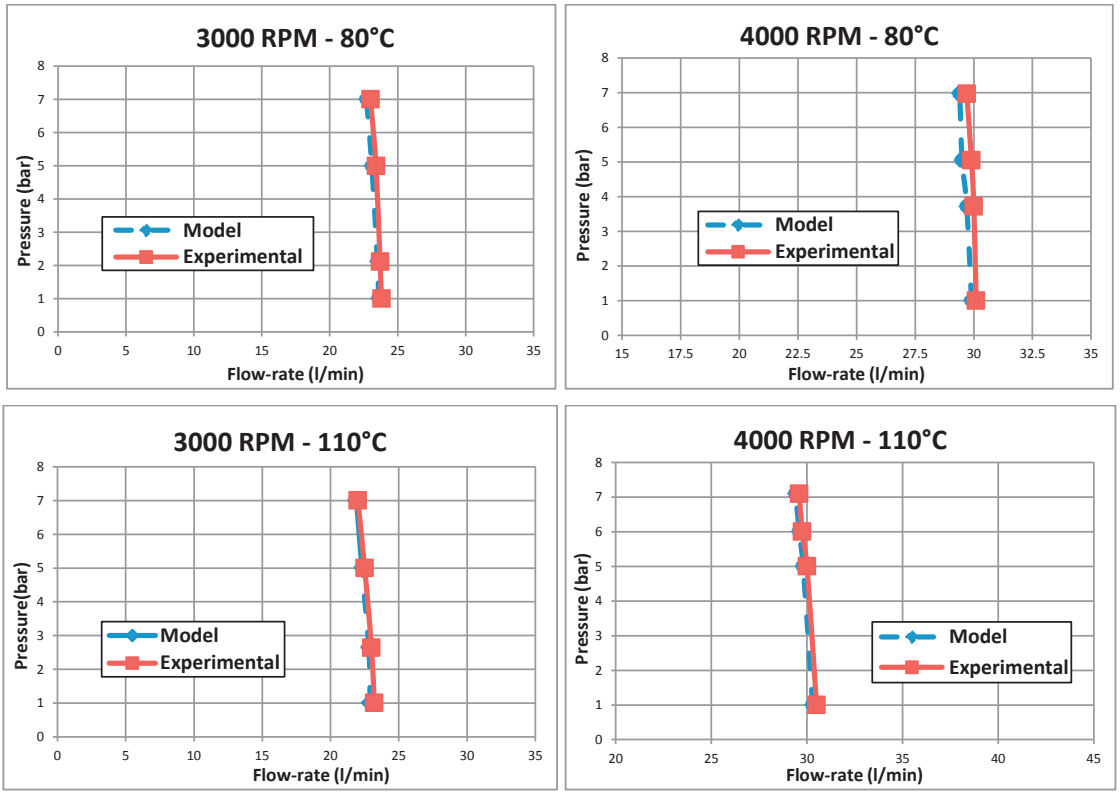

Fig 12. Model/Experiment Results Comparison at 80°C and 110°C oil temperature

From the analysis of the above graphs (figure 12), it can be noted that the numerical model curves slope, with respect to the pressure axis, is very similar to the experimental results. This confirms that the software correctly simulates the pump and captures all main leakages, inter-gears losses and side losses between rotors and pump casing (figure 13).

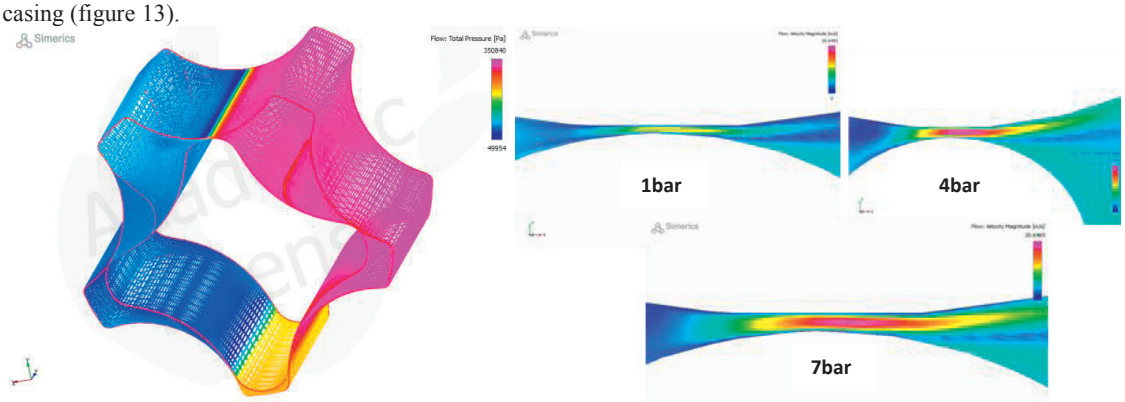

Fig 13. Mean velocity of flow in leakage at 1000rpm

For all the analyzed running conditions, i.e. 1000, 1500, 2000, 2400, 2800 and 3000 rpm rotational speeds, the maximum difference between the model flow-rate data and the experimental one is 9%. This is true also for all the analyzed oil temperatures.

Furthermore, the model allow to study the oil flow – rate behavior versus pump shaft angle. The following figures show the flow-rate trend at two different oil pressures for a pump shaft revolution of 3000rpm.

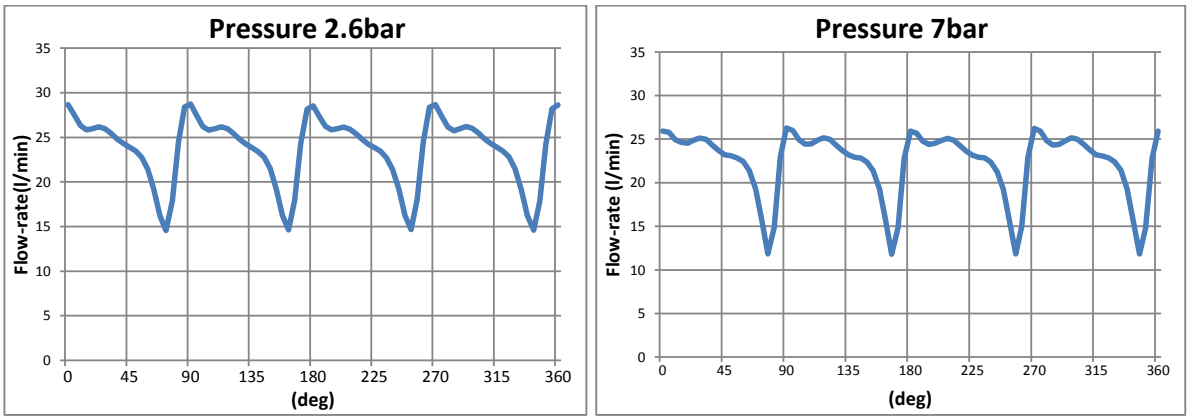

Fig 14. Flow-rate at 3000rpm

5. Conclusion

This paper presents a tridimensional CFD analysis of the oil pump of Aprilia high performance motorbike engine. The pump model was made up with a commercial tri-dimensional code, which allows, starting from the pump geometry, to evaluate the pump performance, taking into account all the phenomena that occurs during the pump operation, including cavitation. The pump model results were compared with experimental data performed in a hydraulic pump test bench of the Department of Industrial Engineering of University of Naples "Federico II", showing a good correlation between experimental and simulated data.

The applied methodology and the model results, led us to conclude that the modeling of a lubrication pump with a CFD 3D commercial code could be an useful instrument to designers to choose the correct pump or to optimize the pump itself.

Acknowledgments

A sincere thanks to OMIQ s.r.l. for technical support.

References

[1] A. Senatore, D. Buono, G. Di Napoli, " Thermo-Fluid-Dynamic Simulated Analysis of a Device for Light Duty Engine Diesel Exhaust Gas After-Treatment System", ASME-ATI-UIT, 2010, Sorrento.
[2] A. Gitt Gehrke, T. Duffe, H. Ding, "Advanced Simulation of the Governing Oil System of an Engine" Stuttgart 2010.
[3] G. W. Stachowiak, A. W. Batchelor,"Engineering Tribology", Butterworth, Heinemann, 2001.
[4] H. Ding, F.C. Visser, Y. Jiang, M. Furmanczyk, "Demonstration and Validation of a 3D CFD Simulation Tool Predicting Pump Performance and Cavitation for Industrial Applications" ASME Technical Paper FEDSM2009 – 78256, 2009, Colorado.
[5] A.K. Singhal, M.M. Athavale, H.Y. Li, Y. Jiang, "Mathematical Basis and Validation of the Full Cavitation Model", Trans. ASME Journal of Fluids Engineering, vol. 124, pp. 617-624, 2002.
[6] A. Senatore, D. Buono, M.V. Prati, M. Manganelli, "Analysis of the Cooling Plant of a High Performance Motorbike Engine", SAE Technical Paper 2012-01-0354, 2012, doi:10.4271/2012-01-0354.
[7] R.E.A. Arndt, "Cavitation in fluid machinery and hydraulic structures," Annual Review of Fluid Mechanics., Vol. 13, pp. 273 – 328, 1981.
[8] F. Bahir, R. Rey, A.G. Gerber, T. Belamri, B. Hutchinson, "Numerical and experimental investigations of the cavitating behavior of an inducer," International Journal of Rotating Machinery, vol. 10, pp. 15-25, 2004.
[9] C.E. Brennen,"Cavitation and Bubble Dynamics", Oxford University Press, 1995.
[10] P. Dupont, T. Okamura, "Cavitating flow calculations in industry," International Journal of Rotating Machinery, vol. 9, pp. 163-170, 2003.
[11] B.E. Launder, D.B. Spalding, "The numerical computation of turbulent flows," Computer Methods, Applied Mechanics and Engineering, vol. 3, pp. 269-289, 1974.
[12] A.K. Singhal, M.M. Athavale, H.Y. Li, Y. Jiang, "Mathematical basis and validation of the full cavitation model", Trans. ASME Journal of Fluids Engineering, vol. 124, pp. 617-624, 2002.
[13] D. Zhang, C.Y. Perng, M. Laverty, "Gerotor Oil Pump Performance and Flow/Pressure Ripple Study" SAE Technical Paper 2006-01-0359, 2006.
[14] Y. Jiang, C.Y. Perng, "An Efficient 3D Transient Computational Model for Vane Oil Pump and Gerotor Oil Pump Simulation," SAE-70841.

[15] M. Fabiani, "Modelling and Simulation of Gerotor Gearing in Lubrication Oil Pumps.", SAE paper 99P-464;
[16] D. Buono, M. Cardone, A Senatore, L .Fabbri *"Analisi Teorico-Sperimentale di un Sistema di Raffreddamento di un MCI per Uso Motociclistico Altoprestazionale"* MISMAC IX - Metodi di Sperimentazione sulle Macchine, Trieste, 24 marzo 2006;
[17] D. Buono, M. Cardone, A. Dominici, A Senatore *"Analisi Fluidodinamica Simulata di Circuiti di Lubrificazione di Motori Alto-Prestazionali"* MISMAC IX - Metodi di Sperimentazione sulle Macchine, Trieste, 24 marzo 2006;
[18] D. Buono, M. Cardone, A. Senatore, L. Fabbri *"Optimization Methodology of High Performance Motorcycle Engine Cooling System"* FISITA 2006 World Automotive Congress, Yokohama, Japan, October 22-27, 2006;
[19] D. Buono, M. Cardone, A. Senatore, A. Dominici *"Fluid-dynamic Analysis of a High Performance Engine Lubricant Circuit"* SAE paper n. 2007-01-1963 JSAE/SAE International Fuels and Lubricants Meeting, Kyoto, Japan, July 23-27, 2007;
[20] D. Buono, M. Cardone, A. Senatore, E. Pulci Doria, A. Dominici *"Thermo-Fluid-dynamic Analysis of a High Performance Engine CoolingSystem"* SAE paper n. 2007-24-0061 – ICE2007 8th International Conference on Engine for Automobile, Capri, Italy, September 16-20, 2007,
[21] M. Cardone, A. Senatore, D. Buono, M. Gustato, W. Scattolin *"Simulated Analysis of a Motorbike High Performance Lubrication Circuit"* SAE paper n. 2008-01-1647, SAE Powertrains, Fluid, and Lubricants Congress, Shanghai, China, 23-25, June, 2008;
[22] A. Senatore, M. Cardone, D. Buono, C. Pezzella, A. Dominici, E. Pulci Doria *"Analisi Termofluidodinamica del Sistema di raffreddamento di un Motore Altoprestazionale"* 63° Congresso Nazionale ATI, Palermo, 23-26 settembre, 2008;
[23] D. Buono, A.Senatore, M. Cardone, "*Analisi sperimentale di una pompa del circuito di lubrificazione di un motore motociclistico altoprestazionale*" , 65 Congresso nazionale ATI, Cagliari, 13 – 17 settembre 2010;
[24] D. Buono**,** A.Senatore, M. Cardone, C. Lombardi, "*A simulation model of an engine motorbike lubrication circuit",* CONAT 2010 International Congress on Automotive and Transport Engineering, 27-29 October, Brasov, Romania;

Contact information

Emma Frosina
Department of Industrial Engineering, University of Naples Federico II - Via Claudio 21, Naples, Italy
emma.frosina@unina.it
www.dime.unina.it

Definitions/Abbreviations

$\mathbf{S'_{ij}}$	Strain tensor	$\boldsymbol{\rho_l}$	Liquid density (kg/m^3)
U	Initial velocity	$\boldsymbol{\rho_v}$	Vapor density (kg/m^3)
τ	Dimensionless cavitation coefficient	$\boldsymbol{\sigma}$	Surface of control volume
$\boldsymbol{\Omega}$	Control volume	$\boldsymbol{\sigma_k}$	Turbulence model constant
$\boldsymbol{\eta}$	Dynamic viscosity [Pa-s]	$\boldsymbol{\sigma_l}$	Surface tension
$\mathbf{C_c}$	Cavitation model constant	$\boldsymbol{\sigma_\varepsilon}$	Turbulence model constant